BUTTERWORTH HEINEMANN

Polymer Vol. 36 No. 17, pp. 3255–3266, 1995

0032-3861/95/$10.00 + 0.00

Thermal and morphological behaviours of bisphenol A polycarbonate/poly(butylene terephthalate) blends

D. Delimoy*, B. Goffaux, J. Devaux† and R. Legras
Unité de Physique et de Chimie des Hauts Polymères, Université Catholique de Louvain, Croix du Sud 1, B 1348 Louvain la Neuve, Belgium
(Received 19 September 1994; revised 7 February 1995)

Crystallization of bisphenol A polycarbonate/poly(butylene terephthalate) (PC/PBT) blends at low undercoolings ($\leq 60°C$) was first studied in isothermal conditions by rapidly cooling samples from the melt. Differential scanning calorimetry (d.s.c.) half-crystallization times ($t_{1/2}$) were obtained. At the same time, transmission electron microscopy (TEM) analyses were undertaken on microtome sections from quenched and crystallized d.s.c. samples. The d.s.c. behaviour appears to be linked to the dispersion of PBT in the blends. For blends in which PBT is finely dispersed in PC, $t_{1/2}$ lies around 10^3 s. In the reverse situation, the blends, like pure PBT, cannot be quenched, showing a $t_{1/2}$ in the same range as that of the pure polymer. In the co-continuous range, $t_{1/2}$ measurements are not very reproducible. They lie between those of dispersed PC and dispersed PBT blends. On the basis of these observations, original mechanisms of crystallization are proposed. The main feature of these mechanisms is the slowness of the PBT crystallization when it is finely dispersed. This behaviour is attributed to a low nucleation density. Crystallization of PC/PBT blends at high undercoolings was undertaken using d.s.c. cooling experiments. When some PBT is finely dispersed, an exotherm occurs on cooling, well below the T_g of the PC-rich phase. An evolution of T_{ch}, ΔH_{ch} (respectively, crystallization temperature and enthalpy on heating) and ΔH_m (melting enthalpy) as a function of annealing temperature occurs on reheating the samples. Surprisingly enough, a stepwise transition in morphology takes place around 110°C, which is confirmed by the very different microstructures observed by TEM for samples annealed at 105°C and 150°C. A tentative phase diagram is finally proposed which shows that a spinodal-type phase decomposition should occur around 110°C. Competition between a crystallization mechanism involving a homogeneous nucleation step and this spinodal phase decomposition probably takes place. The result is that the homogeneous nucleation mechanism, which is shown to occur in pure PBT when finely dispersed, is delayed until the spinodal decomposition occurs.

(Keywords: blend; polycarbonate; poly(butylene terephthalate))

INTRODUCTION

Simultaneously with the increase in their commercial importance, blends of bisphenol A polycarbonate (PC) and poly(butylene terephthalate) (PBT) have induced numerous scientific investigations. Some papers deal with the chemical stability of these blends in the melt[1–5]. Transesterification has been shown to occur, catalysed by transition metal residues. Organophosphite stabilizers appear to be very efficient in inhibiting these exchange reactions[5–7]. Mechanistic and kinetic studies in this field have led to a better understanding and control of the exchange reactions. In the present work, chemical stabilization is used in order to avoid any transesterification[5,8].

The scientific interest in PC/PBT blends arises from the particular situation of the base polymers, which constitute a rare case of a fast-crystallizing polymer (PBT) that is partially miscible with a second, usually amorphous constituent (PC). This partial miscibility of PC and PBT has already been pointed out by several researchers and should be expected from the closeness of their solubility parameters[9]. The clearest indications of the miscibility have been given by Wahrmund *et al.*[10] and Birley and Chen[11].

Selective staining techniques[12–14], further developed in our laboratory[15] and elsewhere[16], make possible the direct microscopic observation of the phase behaviour of these blends. Therefore, the purpose of this paper is to show how these techniques can be applied in order to analyse the interplay of crystallization and miscibility. The aim is to gain insight into the physical behaviour of PC/PBT blends through a study of the complex structures which can be observed.

The first part of this paper deals with the crystallization rates of PC/PBT blends at low undercoolings ($\leq 60°C$) and their relationship with the corresponding microstructures. Particular characteristics which were

* Present address: Laboratoire Central Solvay, Neder-over-Hembeek, Belgium
† To whom correspondence should be addressed

observed at higher undercoolings (>60°C) will be dealt with in the second part.

EXPERIMENTAL

Polymers

The PBT used was Dynalit PTMT from Dynamit Nobel. Its weight average molecular weight was 110 000. The PC used was Lexan 135 from General Electric. Its weight average molecular weight was 35 000. Before any experiment, PC and PBT were dried at 120°C under vacuum for at least 24 h. The solubility parameters of PC and PBT were determined[9] by calculation to be around 10.0 ± 0.2.

Processing

The processing of PC/PBT blends was achieved in a Brabender W50EH mixer (electrical heating). Mixing was performed at 260°C for 5 min. The temperature and torque inside the melt were recorded. Samples were taken and immediately pressed at 260°C for 2 min, then cooled under pressure in another cold press.

Melt chemical stabilization

Chemical stabilization was effected through melt mixing of 0.5% (w/w) of triphenyl phosphite in each blend. Transesterification levels under 10^{-5} were assessed by infra-red spectroscopy (i.r.), ^1H nuclear magnetic resonance (n.m.r.) and solubility cross-measurements according to the procedures developed in our laboratory[8].

Differential scanning calorimetry (d.s.c.)

Thermal treatments were performed on a Perkin–Elmer DSC7 system previously standardized by the use of several low-melting metals.

For analyses at low undercoolings, samples (between 5 and 20 mg) were first melted at 260°C for 2 min, then cooled at a maximum rate (150°C min^{-1}) down to the isothermal crystallization temperature. The zero time was taken when the setting temperature was reached within the d.s.c. cell. The half-crystallization time ($t_{1/2}$) was measured at the peak of the crystallization exotherm.

For analyses at high undercoolings, normal isothermal procedures could not be applied, owing to the thermal inertia of the d.s.c. oven. Therefore, before the d.s.c. analyses, samples (between 5 and 20 mg) were melted for 2 min at 260°C in sealed aluminium cups, then quenched in iced acetone.

Standard cycles at high undercoolings included a first heating step (10°C min^{-1}) up to 260°C followed by a cooling step at a controlled rate (10°C min^{-1}) down to −20°C, then a second heating step (10°C min^{-1}) up to 260°C. Glass transition temperatures (T_g) were defined at the midpoints of the specific heat steps, while crystallization temperatures on heating (T_{ch}), on cooling (T_{cc}), and melting temperatures (T_m) were defined at the maxima or minima of the d.s.c. peaks. The corresponding enthalpy changes (ΔH_{ch}, ΔH_{cc} and ΔH_m) were obtained from peak area integrations.

For the annealing experiments, samples were first melted at 260°C for 2 min, then cooled at a maximum rate (150°C min^{-1}) down to the isothermal annealing temperature. After annealing, samples were reheated at 10°C min^{-1}.

Transmission electron microscopy (TEM)

Ultrathin sections of samples annealed in the d.s.c. cell were performed at room temperature using a LKB Ultratome 3 device fitted with a diamond knife. The ultrathin sections (30–50 nm thick) were recovered on a 400 mesh Cu–Rh grid. As already reported[15] the natural contrast between PC and PBT phases is very weak. Sections were thus stained by being exposed to RuO_4 vapours for 7–10 min following a procedure previously described[15].

The microscope was a Philips EM301. Thin foil diaphragms of 10 μm or 100 μm diameter were used. The acceleration voltage used was between 60 and 80 kV.

Optical microscopy (OM)

Thin films were cast from a 50/50 CH_2Cl_2/CF_3COOH solvent mixture. The films were annealed in a Mettler FP5 hot stage. After annealing, the samples were quenched in cold water. The microscope was an Orthoplan POL from Leitz used with polarized light.

Scanning electron microscopy (SEM)

Samples that were analysed by SEM were gold plated in a Balzers Union SCD 040 device. The microscope was a Hitachi S-570 working at an acceleration voltage between 10 and 25 kV.

Etching of some sample surfaces with CH_2Cl_2, which selectively dissolves PC, was attempted in order to reveal the surface microstructure.

RESULTS AND DISCUSSION:
1. LOW UNDERCOOLINGS

Microstructure after quenching

As already pointed out in the literature[10,11,17,18], PC and PBT show partial miscibility. *Figure 1* reports the glass transitions observed by d.s.c. for PC/PBT blends quenched from 260°C and heated again at 10°C min^{-1}.

At low PBT contents (<8% by weight), only one T_g is observed. Its value decreases from 147°C (pure PC) to 135 ± 5°C for the 92.5/7.5 PC/PBT blend. TEM study of these blends confirms that they are monophasic and amorphous after quenching from 260°C (*Figure 2*).

For the blends which contain more than 80% PBT, only one T_g can be seen (*Figure 1*). The position of this T_g is very close to the PBT glass transition (~42°C).

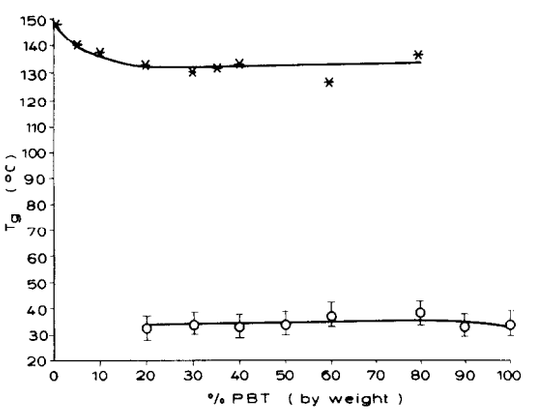

Figure 1 Glass transition temperature (T_g) of PC-rich (*) and PBT-rich (O) phases as a function of blend composition

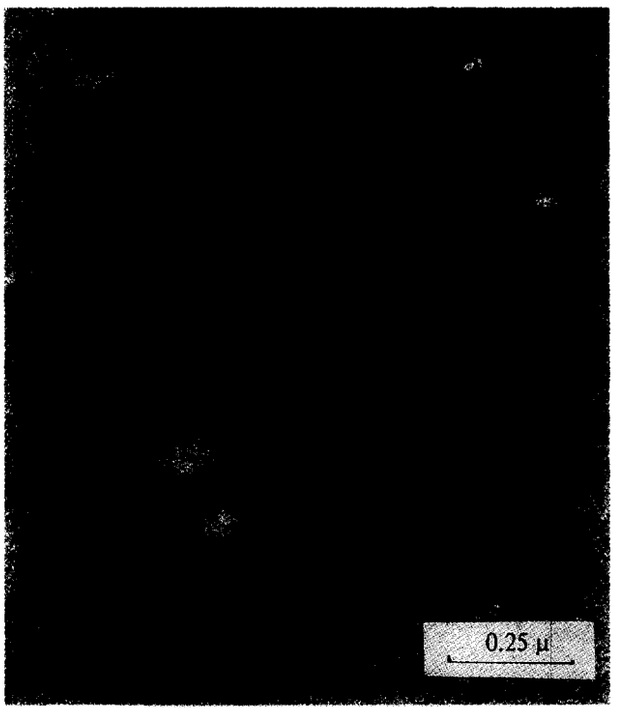

Figure 2 TEM micrograph of a 92.5/7.5 PC/PBT blend after melting for 2 min at 260°C then quenching in iced water

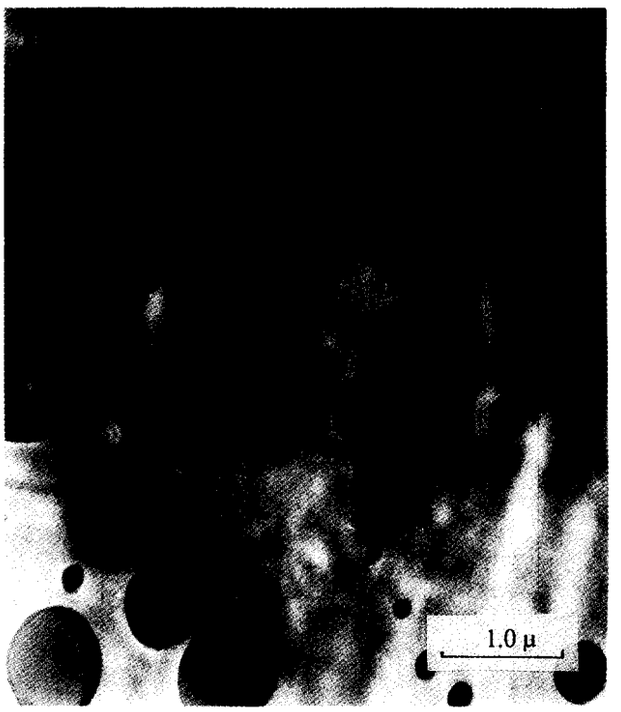

Figure 4 TEM micrograph of a 20/80 PC/PBT blend after melting for 2 min at 260°C then quenching in iced water

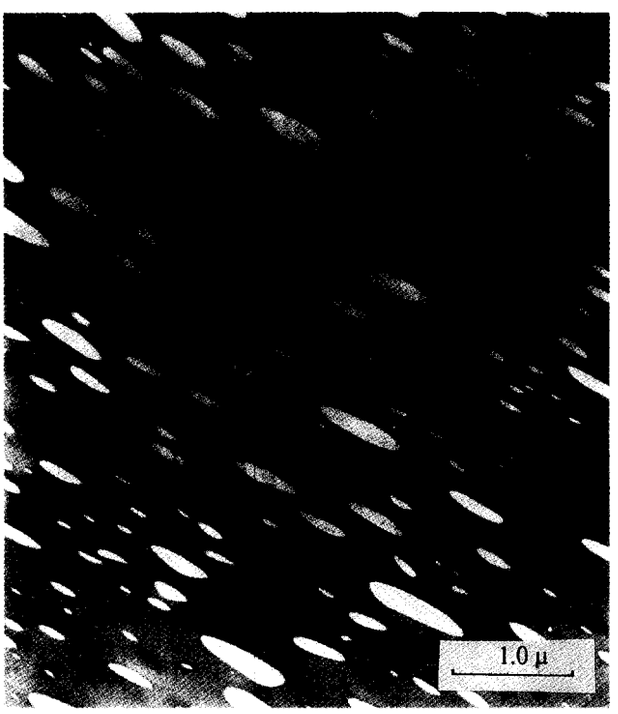

Figure 3 TEM micrograph of an 80/20 PC/PBT blend after melting for 2 min at 260°C then quenching in iced water

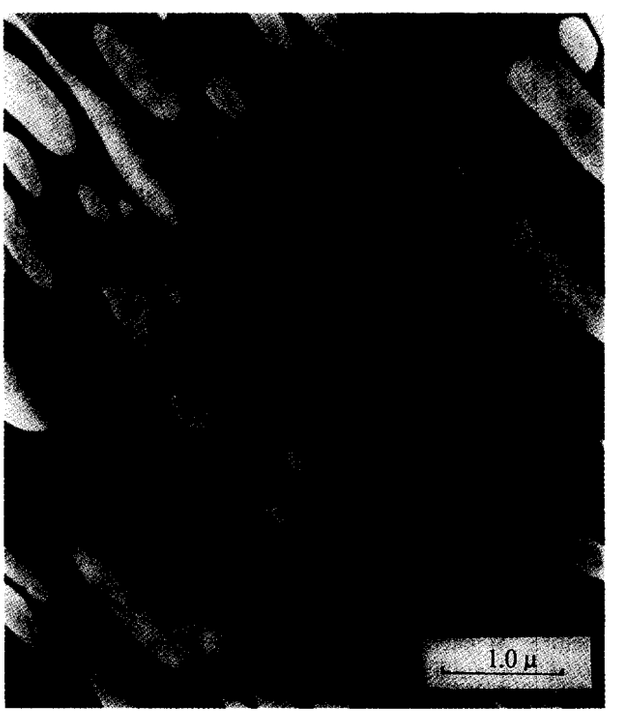

Figure 5 TEM micrograph of a 60/40 PC/PBT blend after melting for 2 min at 260°C then quenching in iced water

However, TEM observations reveal that blends containing up to 90% PBT still include a dispersed second phase. Therefore, it was concluded that the miscibility of PC in PBT is certainly below 10%, which corresponds to values reported in the literature[18]. Blends containing 95% PBT appear to be homogeneous by TEM.

Two phases are observed by TEM for blends containing between 8 and 90% PBT after being quenched from the melt (260°C). The structures range from a continuous PC-rich phase for compositions with between 8 and 35% PBT (*Figure 3*) to a continuous PBT-rich phase for compositions with between 50 and 90% PBT (*Figure 4*). Compositions with between 35 and 50% PBT exhibit large phases (*Figure 5*). All PC/PBT blends containing 8–90% PBT are biphasic.

Crystallization kinetics of PC/PBT blends

A series of experiments was undertaken in order

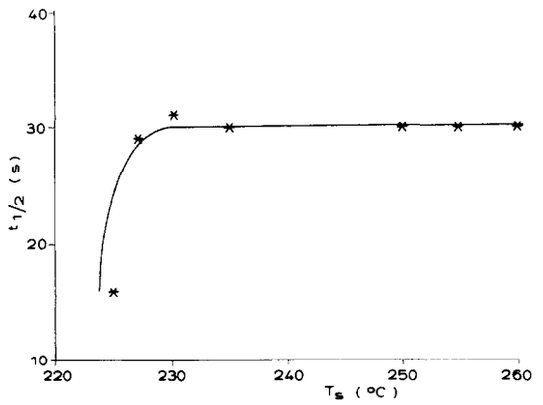

Figure 6 Half-crystallization time ($t_{1/2}$) at 195°C as a function of melting temperature (T_s) for PBT melt mixed for 5 min at 260°C with 0.5% of triphenyl phosphite (TPP)

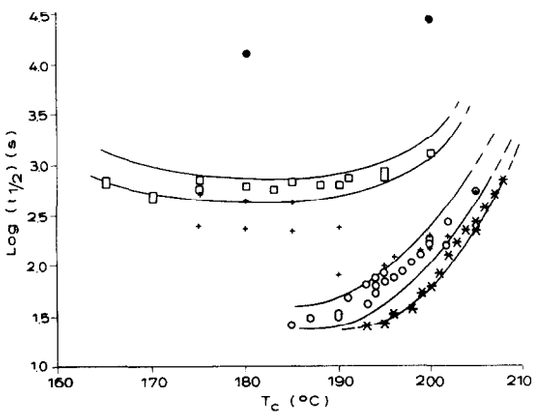

Figure 7 Half-crystallization times ($t_{1/2}$) for PBT in PC/PBT blends as a function of crystallization temperature (T_c): (*) pure PBT (with and without 0.5% TPP); (O) PC/PBT composition with above 50% PBT; (+) PC/PBT compositions with between 35 and 50% PBT; (□) PC/PBT compositions with between 8 and 35% PBT; (●) PC/PBT compositions with below 8% PBT

to determine the minimum melting temperature (T_s) necessary to delete any thermal history from the samples. *Figure 6* shows the half-crystallization times ($t_{1/2}$) of pure PBT recorded at 195°C after 5 min at increasing 'melting' temperatures T_s. The results show that 5 min at a T_s just above 230°C would stabilize $t_{1/2}$. This temperature corresponds to the extrapolated thermodynamic melting temperature of PBT[8]. However, as the processing temperature of the blends was 260°C, preference was given to this temperature for the melting of each sample. It was verified that 2 min at 260°C was sufficient to stabilize $t_{1/2}$ (measured at 195°C) at a value of 30 s.

Figure 7 reports the temperature dependence of $t_{1/2}$ for the full range of analysed PC/PBT blends. The results for pure PBT (melt mixed with 0.5% by weight of the transesterification inhibitor triphenyl phosphite) are also reported for comparison.

Homogeneous blends (containing less than 8% PBT by weight) show a very low crystallization rate from the melt, with $t_{1/2}$ values as high as 10^4 s. Hereafter, they will be referred to as 'PBT dissolved in PC'.

Heterogeneous blends with a continuous PC-rich phase after quenching (between 8 and 35% PBT) will be called 'PBT dispersed in PC'. These blends show $t_{1/2}$ values of about 10^3 s in the full range of crystallization temperatures between 200 and 165°C.

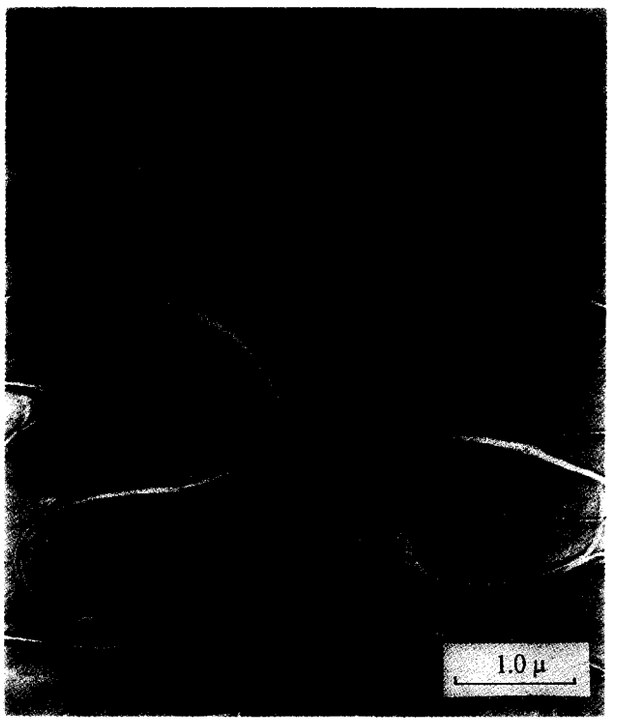

Figure 8 TEM micrograph of a 95/5 PC/PBT blend melted for 2 min at 260°C, quickly cooled (150°C min^{-1}) to 200°C and crystallized at that temperature for 600 min before quenching in iced water

Blends characterized by a continuous PBT-rich phase show $t_{1/2}$ values in the same range as for pure PBT. It should be noted that their crystallization rates are too high to allow $t_{1/2}$ measurements below 185°C. Moreover, like pure PBT, these blends cannot be quenched down to an amorphous state, prohibiting $t_{1/2}$ measurements from the glassy state. They will be called hereafter 'PC dispersed in PBT'.

Finally, the $t_{1/2}$ values of the blends containing 35–50% PBT (PC/PBT blends in the co-continuous range) lie between the two above-mentioned $t_{1/2}$ ranges. However, the crystallization exotherms are broad, leading to poor reproducibility in the determination of the peak value. In one of the cases, two broad maxima were observed.

The above-described thermal behaviour of the two-phase PC/PBT blends (containing 8–90% PBT) could hardly be predicted from the TEM microstructures of the quenched blends reported earlier. It is particularly difficult to understand why the PBT-rich phase in the different kinds of blends crystallizes in such a wide range of $t_{1/2}$ values (from a few seconds to 10^3 s) at the same temperature. TEM analyses of crystallized blends were therefore undertaken in order to find out the reasons for this behaviour.

TEM studies of crystallized blends

PBT dissolved in PC. A blend in which PBT was dissolved in PC (5% PBT by weight) was crystallized from the melt at 200°C for 600 min. This prolonged treatment at the crystallization temperature (T_c) was necessary because of the very low crystallization rate of

the homogeneous blends. The TEM structure observed on a section cut with an ultramicrotome out of a d.s.c. sample is reported in *Figure 8*. A loose network of crystalline PBT lamellae (clear) can be seen embedded in a continuous PC-rich (dark) phase. The very long crystallization annealing at 200°C results in large lamellae. They appear to be several micrometres long and around 50 nm thick. They are curved and show many branching points. Precise microscopic observation shows that the lamellae are bordered by a darker zone. As the darkening is the result of the selective staining of the PC molecules with RuO_4[15], it can be assumed that this zone is enriched in PC.

The very low rate of overall crystallization for this class of blends can be attributed to the slow diffusion of PBT molecules through the PC-rich phase, which seems to limit the growth rate of the lamellae. The results of Hobbs *et al.*[19] seem to support a significant but slow diffusion of PBT within a PC phase at 200°C. The diffusion-controlled crystallization mechanism proposed here seems to be slowed down by the lack of crystallizable species within the growth front (depletion layer[20]).

PBT dispersed in PC. For the second class of blends, characterized by PBT-rich nodules dispersed in a PC-rich phase (*Figure 3*), abnormally high $t_{1/2}$ values are seen on isothermal annealing. Thus, a sample of 80/20 PC/PBT blend was crystallized for a period far longer than $t_{1/2}$, cut with an ultramicrotome in thin sections and observed by TEM. Its microstructure (*Figure 9*) shows a dense network of lamellae packed into large intersections and regularly dispersed in the continuous PC-rich phase. These intersection zones look like the well-defined nodules observed in the quenched sample (*Figure 3*). TEM analysis of such a sample after a crystallization time shorter than $t_{1/2}$ (*Figure 10*) reveals two distinct regions. The first one is identical to the structure of the sample crystallized over a long time (*Figure 9*), while the second region is similar to the quenched structure (*Figure 3*). The border between the two regions suggests that the crystallization of the PBT-rich nodules occurs when they are nucleated by lamellae growing in the PC-rich phase.

Thus, the first step of the crystallization mechanism, which is rate determining, appears to involve the growth of PBT lamellae from the 'crystalline' region of the sample to the 'amorphous' one through the PC-rich continuous phase. A second and faster step occurs when a lamella runs across a PBT-rich nodule. Owing to its high PBT concentration and the undercooling, the latter crystallizes rapidly and gets deformed, giving rise to several new lamellae which start to grow into the PC-rich continuous domain.

As the first step, i.e. the crystallization of PBT dissolved in PC, is the rate-determining one, the overall crystallization is slow. The second step, i.e. the fast crystallization of the nodules, provides only a small positive contribution to the overall crystallization rate.

It is important to note that the PBT-rich phase when dispersed in small nodules shows a much slower crystallization rate than in extended domains. An explanation of this behaviour can be found in the nucleation density of PBT, which can be calculated from the mean spherulitic diameter observed in pure

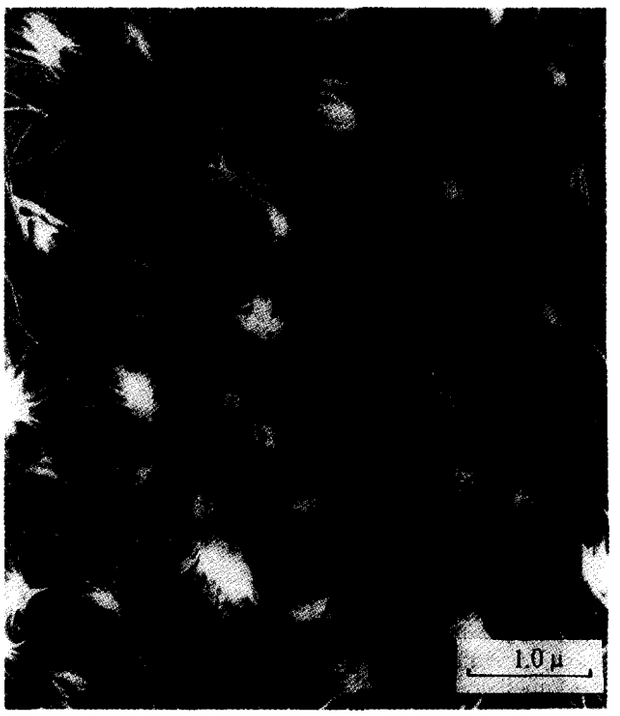

Figure 9 TEM micrograph of an 80/20 PC/PBT blend melted for 2 min at 260°C, quickly cooled (150°C min^{-1}) to 200°C and crystallized at that temperature for 60 min before quenching in iced water

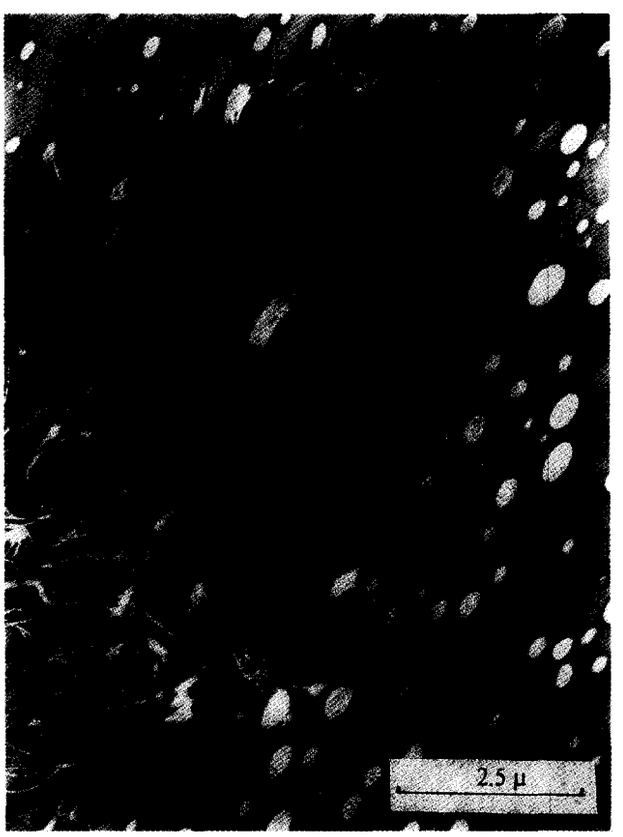

Figure 10 TEM micrograph of an 80/20 PC/PBT blend melted for 2 min at 260°C, quickly cooled (150°C min^{-1}) to 200°C and crystallized at that temperature for 8 min before quenching in iced water

PBT (5–10 μm). The calculation leads to a nucleation density in the range $1.9 \times 10^9 - 1.5 \times 10^{10}$ cm^{-3}. As the mean diameter of a PBT-rich nodule in an 80/20 PC/PBT blend is in the range 0.2–1 μm, one nodule in every 100 at the very maximum contains a nucleating species. The PBT-rich nodules can therefore be compared to the droplets of crystallizable polymer reported by other authors[21–23] to show also a significant decrease in the crystallization rate. A detailed study of the thermal behaviour at high undercoolings for blends made from PBT dispersed in PC will be presented later.

PC dispersed in PBT. The TEM micrograph of a blend consisting of PC dispersed in PBT (20/80 PC/PBT) is shown in *Figure 11*. It shows a continuous crystalline PBT phase where distinct lamellae can clearly be observed. Note that the fine morphology appears clearer than in pure PBT where the lamellar structure is usually not observed by TEM at the same magnification. It is thus assumed that PC molecules are excluded from the PBT lamellae within the PBT-rich phase. They concentrate at the edge of the lamellae and are stained by RuO_4 treatment, providing a well-contrasted picture of the lamellae.

In the case of these blends, the crystallization of PBT within the continuous PBT-rich phase does not suffer from a low nucleation density, owing to the high growth rate of the crystalline species. By comparison with pure PBT, the above-described PC exclusion only slows down the crystallization to a limited extent. This could explain why these blends, like PBT, cannot be quenched in the d.s.c. experiments.

In *Figure 11*, owing to the long crystallization time, the dispersed PC-rich (dark) phase appears to be streaked with clear lamellae which witness that the PBT molecules dissolved in the PC-rich phase also crystallize, but at a fairly low rate. These lamellae grow from the interface where the crystalline PBT-rich phase provides nucleation sites in abundance.

Figure 11 TEM micrograph of a 20/80 PC/PBT blend melted for 2 min at 260°C, quickly cooled (150°C min^{-1}) to 200°C and crystallized at that temperature for 60 min before quenching in iced water

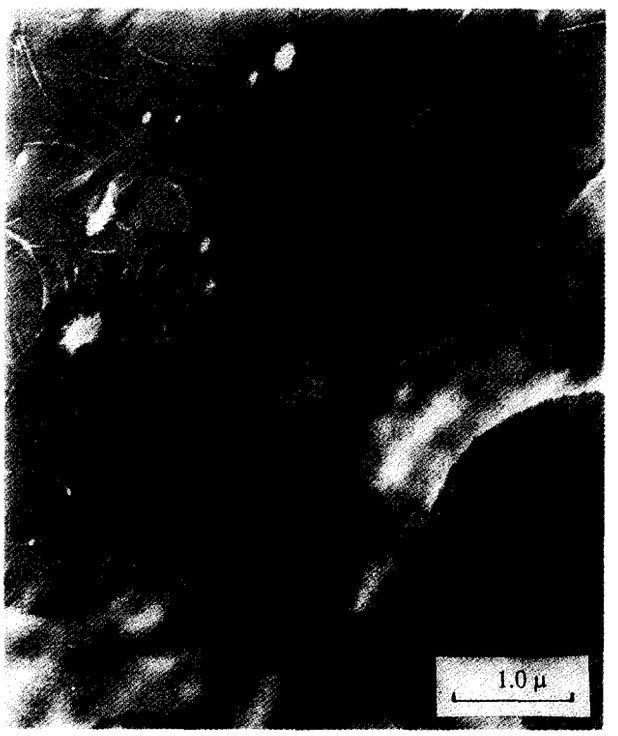

Figure 12 TEM micrograph of a 60/40 PC/PBT blend melted for 2 min at 260°C, quickly cooled (150°C min^{-1}) to 180°C and crystallized at that temperature for 15 min before quenching in iced water

Figure 13 TEM micrograph of a 60/40 PC/PBT blend melted for 2 min at 260°C, quickly cooled (150°C min^{-1}) to 200°C and crystallized at that temperature for 2 min before quenching in iced water

PC/PBT blends in the co-continuous range. *Figures 12* and *13* show two TEM micrographs of 60/40 PC/PBT samples after different crystallization treatments. In *Figure 12*, which shows a sample crystallized for a period of time much longer than $t_{1/2}$, two regions are observed. The first one is a fully crystallized PBT-rich zone, while the second region consists of large PC-rich domains in which PBT lamellae growing from the interfaces are observed. *Figure 13* shows the microstructure of a similar sample crystallized for a shorter period of time. Again, the large PBT-rich domains are fully crystallized upon annealing, but the majority of the small PBT-rich nodules are not. As already explained, these nodules show a very low nucleation density, and only those which are crossed by a lamella growing from the PC/PBT interface undergo crystallization.

From these observations, it seems clear that two crystallization rates, and thus two values of $t_{1/2}$, should be observed. Indeed, the d.s.c. results indicated that the behaviour of this class of blends is between those of systems characterized by either a PBT-rich or a PC-rich dispersed phase. However, in the d.s.c. experiments $t_{1/2}$ was approximated by the maximum of the crystallization exotherm. As these exotherms are very broad, the observation of two distinct maxima on the same thermogram remained an exception.

OM and SEM studies of crystallized blends

Analyses by optical microscopy and scanning electron microscopy were also undertaken on blends of PC dispersed in PBT and PBT dispersed in PC.

Observation under a polarized optical microscope of a 20/80 PC/PBT blend after a short crystallization period gives evidence of a spherulitic superstructure (*Figure 14*). The diameters of the spherulites reach 20–30 μm at the end of the crystallization. They are thus by far larger than the diameter of the dispersed PC-rich nodules (1–2 μm diameter; see *Figure 4*). Therefore, these PC-rich nodules should be looked for either within the spherulites, between the radiant fibrils, or outside the spherulites, concentrated close to their boundaries. No evidence for either situation was found by OM. However, SEM studies (not shown) after etching of the PC-rich phase indicated that some segregation of PC-rich nodules to the boundaries of the spherulites should occur.

Parallel studies were also undertaken for an 80/20 PC/PBT blend. Birefringent zones are indeed observed under a polarized optical microscope (*Figure 15*), but there is no Maltese cross to indicate a spherulitic superstructure. SEM observations were questionable owing to the collapse of the microstructure after etching of the PC-rich phase. It can be deduced from both OM and SEM observations of 80/20 PC/PBT crystallized films that no spherulitic superstructure can develop for this composition.

RESULTS AND DISCUSSION: 2. HIGH UNDERCOOLINGS

Thermal analysis of 'PBT dispersed in PC' samples

In the first part of this paper, blends containing between 8 and 35% PBT by weight were shown to contain finely dispersed PBT-rich nodules. These nodules crystallize at a rate which appears exceptionally slow on

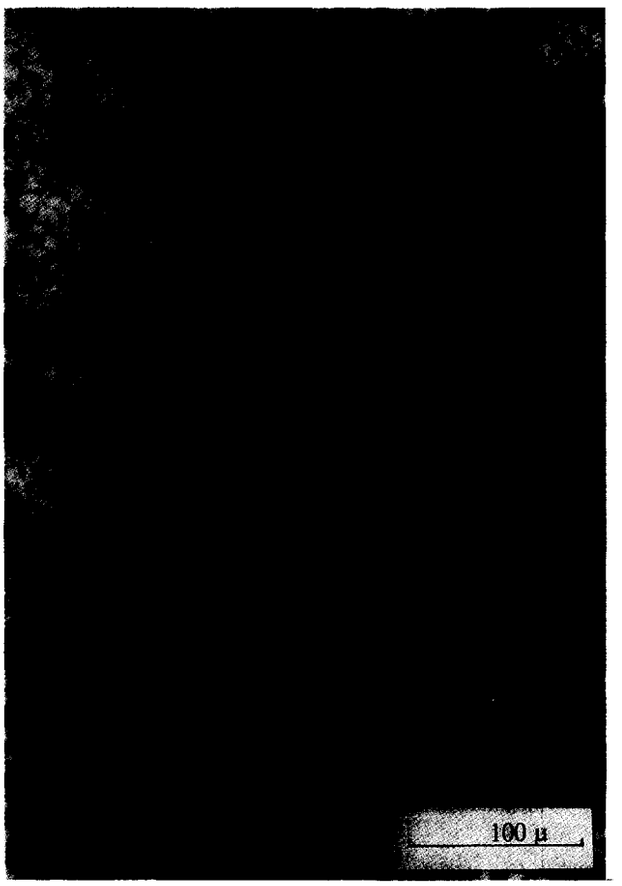

Figure 14 OM micrograph under polarized light of a 20/80 PC/PBT blend melted for 2 min at 260°C, quickly cooled to 190°C and crystallized at that temperature for 30 s before quenching in iced water

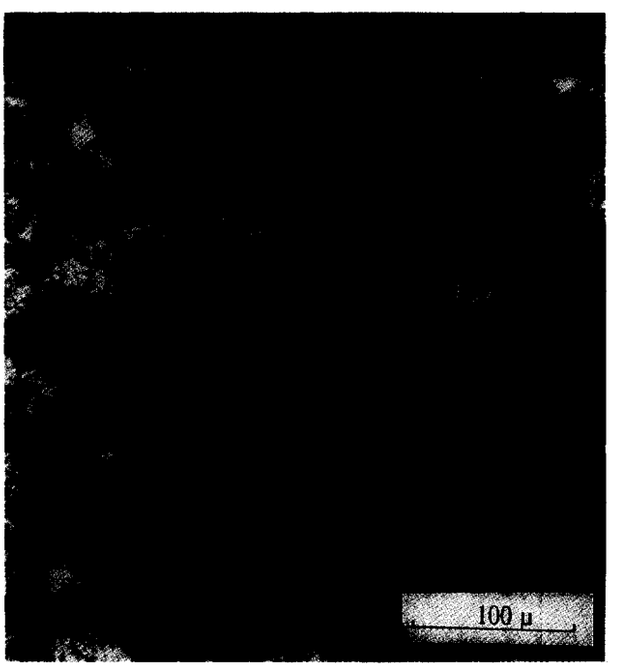

Figure 15 OM micrograph under polarized light of an 80/20 PC/PBT blend melted for 2 min at 260°C, quickly cooled to 208°C and crystallized at that temperature for 40 min before quenching in iced water

account of their high PBT content (around 90%). This was explained in terms of the low nucleation density of PBT. A limited number of fine PBT-rich nodules were also observed in blends in the co-continuous range of compositions (between 35 and 50% PBT by weight). These nodules were also shown to crystallize slowly.

Therefore, owing to the fast crystallization of pure PBT, it was particularly interesting to analyse the thermal behaviour of these two kinds of heterogeneous blends at high undercoolings.

Figure 16 shows the thermogram obtained during the first heating step ($10°C\,min^{-1}$) of the standard d.s.c. cycle for an 80/20 PC/PBT blend together with the analogous PBT thermogram for comparison. Two T_g values are observed, corresponding to the two phases of the blend. Just above these transitions, weak exotherms seem to witness residual PBT crystallization. The melting endotherm is situated at the same temperature as the one for PBT.

For the blends in the co-continuous range of compositions, the first heating thermograms are very similar to those for blends with a dispersed PBT-rich phase.

Figure 17 shows the thermogram obtained during the cooling step for an 80/20 PC/PBT sample (dispersed PBT) and *Figure 18* shows the same thermogram for a 60/40 PC/PBT blend (co-continuous range).

In *Figure 17* there is no crystallization exotherm in the normal range of PBT crystallization (190°C). However, a crystallization exotherm is observed below the T_g of the PC-rich phase ($135 \pm 5°C$) at about 102°C. In *Figure 18* the same unexpected low temperature crystallization exotherm (105°C) can be seen together with a high temperature one (187°C) in the normal range for PBT crystallization on cooling. As the crystallization exotherms at high undercoolings are observed below the T_g of the PC-rich phase, they concern necessarily the PBT-rich phases only.

It appeared impossible in the course of this work to study isothermal crystallization kinetics at high undercoolings owing to the thermal inertia of the d.s.c. cell, which hinders any correct recording of low values of the crystallization enthalpies. Therefore, annealings at different temperatures were performed followed by heating runs with a view to obtaining some values of the crystallinity as a function of annealing time. Two

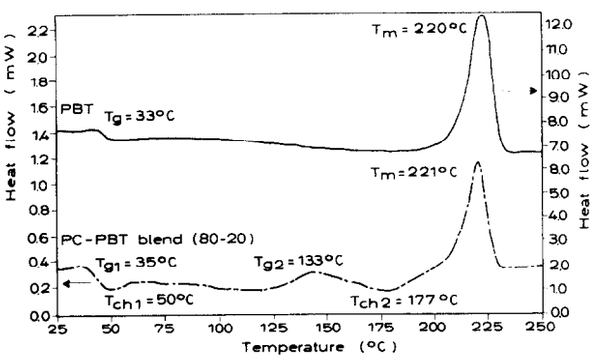

Figure 16 D.s.c. thermograms recorded during the first heating steps ($10°C\,min^{-1}$) for PBT and 80/20 PC/PBT samples

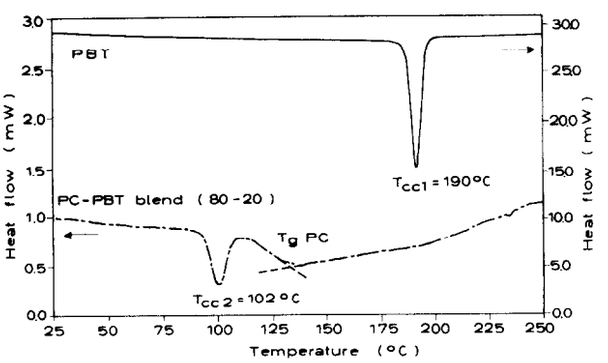

Figure 17 D.s.c. thermograms recorded during the cooling steps ($10°C\,min^{-1}$) from 260°C for PBT and 80/20 PC/PBT samples

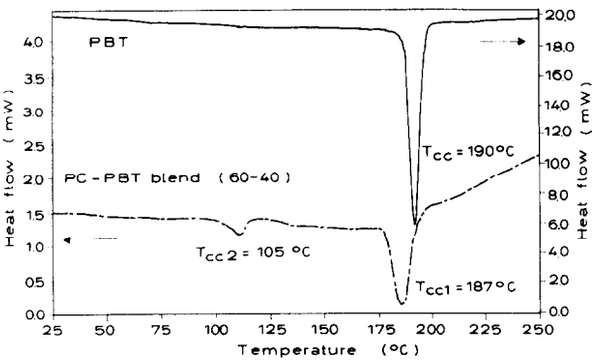

Figure 18 D.s.c. thermograms recorded during the cooling steps ($10°C\,min^{-1}$) from 260°C for PBT and 60/40 PC/PBT samples

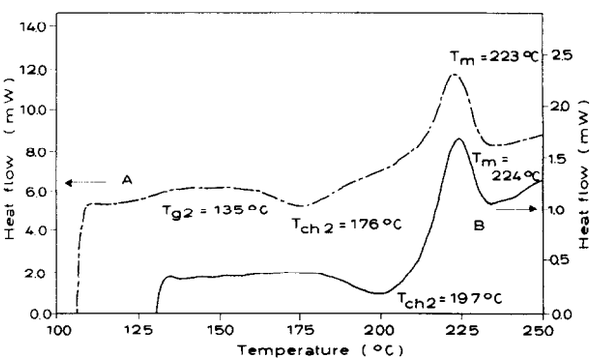

Figure 19 D.s.c. thermograms obtained during the heating step ($10°C\,min^{-1}$) for 80/20 PC/PBT samples annealed for 10 min at 105°C (a) and 150°C (b)

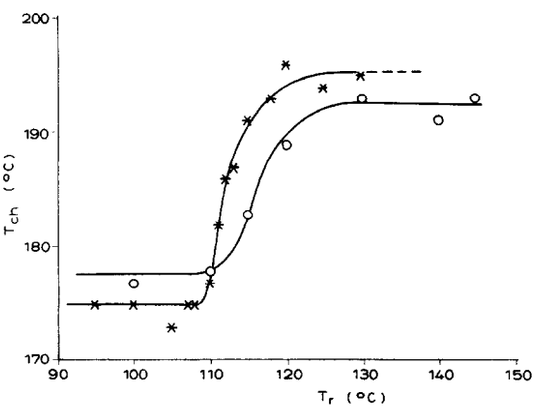

Figure 20 Evolution of T_{ch} as a function of T_r for 80/20 (*) and 70/30 (O) PC/PBT blends (annealing time 2 min)

examples of thermograms obtained during the heating steps of these experiments are reported in *Figure 19*. It can be seen from these thermograms that crystallization on heating depends on the annealing temperature T_r. *Figure 20* reports the stepwise evolution of T_{ch} as a function of T_r for two blend compositions. The crystallization (ΔH_{ch}) and melting (ΔH_m) enthalpies also show this kind of stepwise evolution (*Figures 21* and *22*).

In *Figure 21*, two different types of behaviour can clearly be distinguished. In the range of annealing temperatures above 120°C, ΔH_{ch} and ΔH_m are low and equal. On the contrary, for T_r below 120°C, fairly high ΔH_{ch} and ΔH_m values are obtained. Moreover, a significant difference is observed between ΔH_{ch} and ΔH_m, which means that crystallization is still going on during heating at 10°C min^{-1}. The kinetics are thus markedly enhanced by annealing below 120°C.

Figure 22 shows that the duration of annealing at low temperature has no significant effect on ΔH_m, while the stepwise evolution with annealing temperature T_r is clearly observable around 120°C.

TEM study of 'PBT dispersed in PC' samples

Figure 23 reports a TEM micrograph for an 80/20 PC/PBT sample annealed for 10 min at 105°C then crystallized for 4 min at a T_{ch} corresponding to a maximum crystallization rate (195°C). The picture is remarkably different from the one previously obtained at low undercooling (*Figure 9*). In the present case, all the PBT-rich nodules which are crystalline, as assessed by the d.s.c. analysis, remain very well defined. Radiant lamellae surrounding each nodule are also observed.

From all the above results concerning blends containing finely dispersed PBT-rich nodules, it is obvious that an important transformation occurs within the PBT-rich phase while cooling down to 110°C. The main consequence of this transformation is a quick crystallization of PBT.

RESULTS AND DISCUSSION: 3. THE PC/PBT PHASE DIAGRAM

In order to rationalize the thermal behaviour of PC/PBT blends, a general idea of what could be their phase

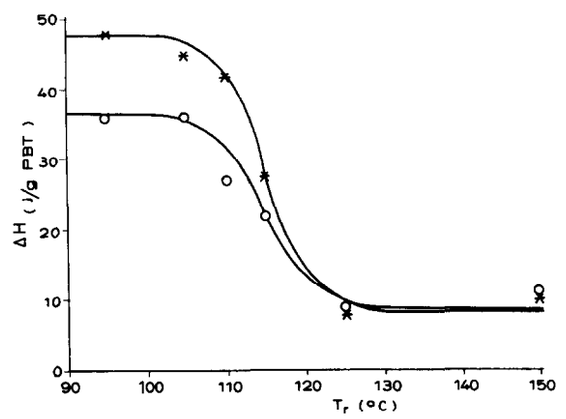

Figure 21 Evolution of ΔH_{ch} (O) and ΔH_m (*) as a function of T_r (10 min) for an 80/20 PC/PBT blend. The enthalpies are normalized to the pure PBT content

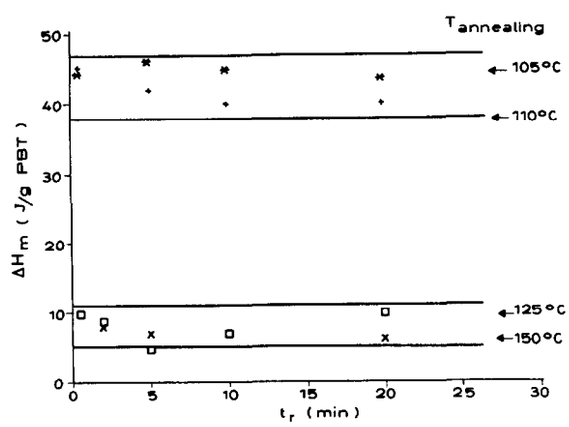

Figure 22 Evolution of ΔH_m for an 80/20 PC/PBT blend as a function of annealing time (t_r) and temperature (T_r). The enthalpies are normalized to the pure PBT content

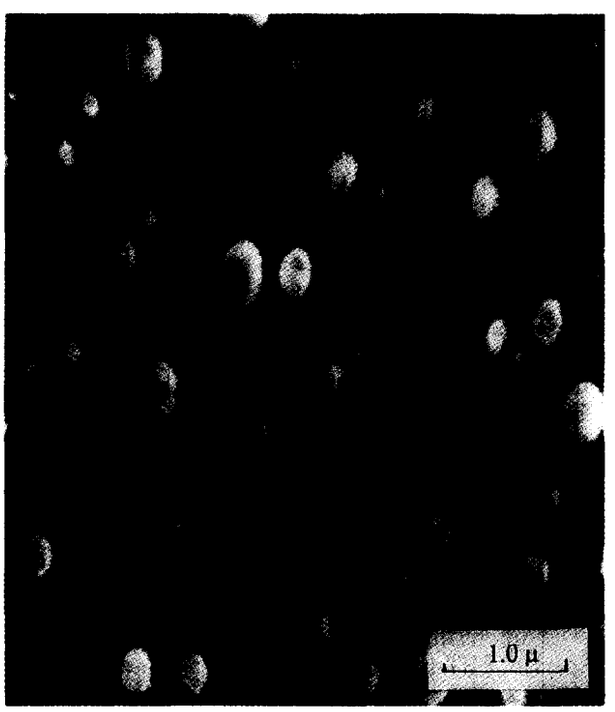

Figure 23 TEM micrograph of an 80/20 PC/PBT blend melted for 2 min at 260°C, quickly cooled (150°C min^{-1}) to 105°C and annealed at that temperature for 10 min, then crystallized at 195°C for 4 min before quenching in iced water

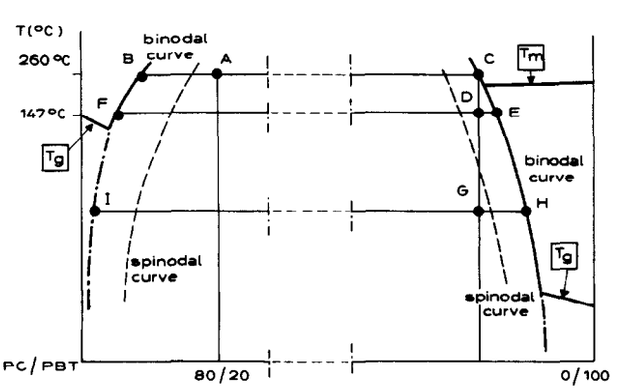

Figure 24 Proposed phase diagram for PC/PBT blends

diagram is necessary. So far, no experimental phase diagram has been published for PC/PBT systems. If we take into account all the observations made here before, it seems that a theoretical 'upper critical solution temperature' (*UCST*) phase diagram can be adapted to the present case.

Schematically, the PC/PBT phase diagram could have the shape represented in *Figure 24*. Its main features would be comparable to the poly(ε-caprolactone)/polystyrene phase diagram proposed by Tanaka and Nishi[24]. However, owing to the chemical instability of PBT and PC/PBT blends at high temperatures, no shape is proposed above 260°C. Therefore, it is not inferred that there is a true *UCST* or an hourglass-type diagram. As this representation is a schematic one, it does not take into account non-regular phenomena due to molecular weight distributions[25] and the lever rule is assumed to be strictly applicable.

In binary polymer systems, when one component is crystallizable, various phase structures can be formed by the competition between the two non-equilibrium phenomena (crystallization and phase separation). Therefore, a melting curve is represented in *Figure 24*, at least on the PBT side of the phase diagram, together with binodal and spinodal curves.

As expected, no significant cryoscopic effect of PC on the melting temperature of PBT was observed in the course of the present work. The melting curve of PBT is therefore drawn almost horizontally. Because no phase transformation is expected to occur below the glass transitions, the binodal and spinodal curves remain hypothetical below the T_g curve.

This classical phase diagram renders an account of the biphasic microstructure of all PC/PBT blends in the range 8–90% PBT by weight. The classical rule of phases predicts that the equilibrium composition of each phase has to remain constant over this full range of concentrations. Following the lever rule, only the size and shape of the phases may vary. Therefore, differences in crystallization rates cannot be rationalized by thermodynamic considerations (equilibrium compositions) but only by kinetic ones, like nucleation differences.

The interesting case of blends containing a finely dispersed PBT-rich phase can be explained from the phase diagram represented in *Figure 24*. For instance, at 260°C, the theoretical composition of an 80/20 PC/PBT blend is represented by point A. As this lies inside the immiscibility domain, the system is separated into two phases (lever rule): a continuous PC-rich phase at point B and a dispersed PBT-rich phase at point C.

When the system is cooled down to 150°C, for instance, point C moves to point D, between the binodal and spinodal curves. A nucleation and growth (NG-type) phase separation can occur inside the nodule, which leads to two new phases represented by E and F, the latter being dispersed in the former. Point D is also situated below the melting curve. The nodule can therefore crystallize if a nucleation seed can be found, but that probability is very low according to the results described earlier. Moreover, if a crystalline seed forms, it will be surrounded by a PC-rich shell (depletion layer), the composition of which will be close to the T_g curve. In consequence, this seed embedded in a nearly glassy shell will probably become inactive as a nucleating site.

If the system is cooled below 110°C, point C moves to point G, which probably lies below both the binodal and spinodal curves. In that unstable region, spinodal decomposition (SD-type) takes place. The characteristics of this SD-type phase separation are the absence of any induction time and the appearance of a periodically modulated microstructure, especially in the initial

Figure 25 TEM micrograph (high magnification) of an 80/20 PC/PBT blend melted for 2 min at 260°C, quickly cooled (150°C min^{-1}) to 150°C and annealed at that temperature for 10 min before quenching in iced water

Figure 26 TEM micrograph (high magnification) of an 80/20 PC/PBT blend melted for 2 min at 260°C, quickly cooled (150°C min^{-1}) to 105°C and annealed at that temperature for 10 min before quenching in iced water

stage[24]. Two new co-continuous phases should therefore appear (points H and I). It is anticipated that the PBT-rich phase crystallizes very quickly. On the other hand, the PC-rich phase (point I) is below the T_g curve and therefore immediately reaches a glassy state. As a consequence, the modulated microstructure should be preserved for a long time after the phase separation.

TEM micrographs of PBT-rich nodules at very high magnifications under annealing conditions corresponding to points D and G are reported in *Figures 25* and *26*, respectively.

When a sample of the 80/20 PC/PBT blend is annealed for 10 min at 150°C, most of the PBT-rich nodules do not show particular substructures. However, a limited number show small PC-rich (dark) micronodules as shown in *Figure 25* (NG-type phase separation).

Upon annealing at 105°C, all the PBT-rich nodules appear to be streaked with very thin dark zones of RuO_4-contrasted PC-rich phase (*Figure 26*) (SD-type phase separation).

The above observations appear to support entirely the mechanism anticipated on the basis of the proposed phase diagram. An SD-type phase decomposition is therefore the most probable transformation undergone around 110°C by blends containing a finely dispersed PBT-rich phase.

However, a particular relationship seems to exist between spinodal phase decomposition and crystal nucleation. Indeed, PBT which, owing to poor nucleation, did not crystallize in the nodules before spinodal phase separation, does subsequently crystallize very quickly. A question thus remains to be answered: can this spinodal decomposition induce nucleation sites or does crystallization, with homogeneous nucleation, precede spinodal decomposition?

In order to solve this problem, a series of experiments was designed in which PBT or a homogeneous 5/95 PC/PBT blend was dispersed in an inert ethylene/propylene (EP) matrix. These blends were submitted to the standard d.s.c. analysis cycle for high undercoolings described earlier. At the same time, the dimensions of the nodules (state of dispersion) were checked by SEM. The results are reported in *Table 1*.

Different T_{cc} values are observed for PBT dispersed in EP. Owing to the large variation in the dimensions of the nodules, the highest T_{cc} can be attributed to those nodules having the larger diameters, which should contain at least one nucleating species.

An unexpectedly high undercooling is observed for the crystallization of the remaining fraction of PBT. This result indicates that low temperature crystal nucleation is not the direct consequence of a spinodal decomposition of the PC/PBT blends, but most probably comes from homogeneous nucleation. However, the low T_{cc} of PBT dispersed in EP remains significantly higher than the T_{cc} obtained in 80/20 PC/PBT. This difference disappears when a 5/95 PC/PBT blend is dispersed in EP instead of PBT only. The PC molecules dissolved in PBT seem to lower the temperature at which the probable homogeneous nucleation of PBT appears. Homogeneous seeds seem to grow only below the spinodal decomposition where a continuous PBT network phase is present in the whole nodule.

Table 1 T_{cc} values of PBT in various dispersion states within an EP matrix

Crystallizable phase	Phase diameter (μm)	T_{cc} (°C)
PBT (bulk)	∞	191
PBT (dispersed)	1.03	194, 132
PBT + 5% PC (dispersed)	1.48	194, 105

CONCLUSIONS

Below 8% and probably above about 90% by weight of PBT, melted PC/PBT blends are monophasic homogeneous systems, while between 8 and 90% PBT the melts appear to be biphasic upon quenching. Below 35% PBT, a PBT-rich phase is dispersed in a PC-rich phase. The reverse situation is observed above 50% PBT. In the range 35–50% PBT, two co-continuous phases can be observed upon quenching.

The half-crystallization times of the blends characterized by a continuous PBT-rich phase can be compared with the pure PBT half-crystallization times. They appear slightly longer owing to the exclusion of PC at the growth front of the lamellae.

The half-crystallization times of PC-rich homogeneous systems are very long as the PBT lamellae are growing within the viscous PC-rich phase.

Surprisingly enough, the half-crystallization times of the two-phase systems where the PBT-rich phase is dispersed remain very long. This appears to be a result of the lack of nucleating species within the dispersed phase. The rate-determining step of the crystallization is therefore similar to the above-described growing of lamellae within a homogeneous PC-rich phase. The crystallization of the dispersed phase (which is a faster step) starts when a lamella hits a PBT-rich nodule which acts thereafter as a seed for new lamellae. This second step is beneficial for the overall crystallization rate. The structure resulting from the two-step crystallization mechanism of these particular systems is a network of PBT lamellae embedded in a PC-rich phase. As the situation before crystallization was a dispersion of PBT-rich nodules, we can describe the resulting structure as a 'crystallization-induced interpenetrated network'.

A major characteristic of the crystallization of the systems in which a PBT-rich phase is finely dispersed is the lack of nucleation in this PBT phase at low undercoolings. This characteristic governs the shape of the final microstructure.

Very different phenomena occur at high undercoolings. The low heterogeneous nucleation of PBT results in a delayed crystallization upon cooling of the blends. An exotherm is observed by d.s.c. below 110°C, well below the glass transition of the PC-rich phase. The crystallization is thought to result from a homogeneous PBT nucleation which becomes effective at such high undercoolings. This is followed by a very rapid growth of the crystals.

The interplay of this mechanism of crystallization with phase separation can be explained by the use of a proposed phase diagram. A spinodal decomposition which should occur around 110°C could delay the crystallization in PC/PBT blends in comparison to

the crystallization of finely dispersed PBT in an inert matrix.

This first insight into the phase diagram of PC/PBT blends seems to promise further interesting research in this field of material science.

ACKNOWLEDGEMENTS

The authors wish to thank Dr R. Koningsveld for reading this manuscript and for his helpful comments on the phase diagram.

REFERENCES

1 Devaux, J., Godard, P. and Mercier, J. P. *J. Polym. Sci., Polym. Phys. Edn* 1982, **20**, 1875
2 Devaux, J., Godard, P., Mercier, J. P., Touillaux, R. and Dereppe, J. M. *J. Polym. Sci., Polym. Phys. Edn* 1982, **20**, 1881
3 Devaux, J., Godard, P. and Mercier, J. P. *J. Polym. Sci., Polym. Phys. Edn* 1982, **20**, 1895
4 Devaux, J., Godard, P. and Mercier, J. P. *J. Polym. Sci., Polym. Phys. Edn* 1982, **20**, 1901
5 Devaux, J., Godard, P. and Mercier, J. P. *Polym. Eng. Sci.* 1982, **22**, 229
6 Golovoy, A., Cheung, M. F., Carduner, K. R. and Rokosz, M. J. *Polym. Bull.* 1989, **21**, 327
7 Golovoy, A., Cheung, M. F., Carduner, K. R. and Rokosz, M. J. *Polym. Eng. Sci.* 1989, **29**, 1226
8 Delimoy, D. PhD Thesis, Louvain la Neuve, 1988
9 Devaux, J. PhD Thesis, Louvain la Neuve, 1979
10 Wahrmund, D. C., Paul, D. R. and Barlow, J. W. *J. Appl. Polym. Sci.* 1978, **22**, 2155
11 Birley, A. W. and Chen, X. Y. *Br. Polym. J.* 1984, **16**, 77
12 Vitali, R. and Montani, E. *Polymer* 1980, **21**, 1220
13 Trent, J. S., Schenbeim, J. I. and Cauchman, P. R. *J. Polym. Sci., Polym. Lett. Edn* 1981, **19**, 315
14 Trent, J. S., Schenbeim, J. I. and Cauchman, P. R. *Macromolecules* 1983, **16**, 589
15 Delimoy, D., Bailly, C., Devaux, J. and Legras, R. *Polym. Eng. Sci.* 1988, **28**, 104
16 Hobbs, S. Y., Dekkers, M. E. J. and Watkins, V. H. *J. Mater. Sci.* 1988, **23**, 1219
17 Hanrahan, B. D., Angeli, S. R. and Runt, J. *Polym. Bull.* 1985, **14**, 399
18 Kim, W. N. and Burns, C. M. *Makromol. Chem.* 1989, **190**, 661
19 Hobbs, S. Y., Watkins, V. H. and Bendler, J. T. *Polymer* 1990, **31**, 1663
20 Wang, T. T. and Nishi, T. *Macromolecules* 1977, **10**, 421
21 Hoffmann, J. D., Frolen, L. J., Ross, G. S. and Lauritzen, J. I. *J. Res. Nat. Bur. Stand., Sect. A* 1975, **79**, 671
22 Chever, R. A., Barham, P. S., Martinez-Salazar, J. and Keller, A. *J. Polym. Sci., Polym. Phys. Edn* 1982, **20**, 1717
23 Barham, P. S., Jarvis, D. A. and Keller, A. *J. Polym. Sci., Polym. Phys. Edn* 1982, **20**, 1733
24 Tanaka, H. and Nishi, T. *Phys. Rev. Lett.* 1985, **55**, 1102
25 Koningsveld, R., Solc, K. and MacKnight, W. J. *Macromolecules* 1993, **26**, 6676